Chapter 5
Flexible-Link Robots

Abstract Control for flexible-link robots is a non-trivial problem that has elevated difficulty comparing to the control of rigid-link manipulators. This is because the dynamic model of the flexible-link robot contains the nonlinear rigid link motion coupled with the distributed effects of the links' flexibility. This coupling depends on the inertia matrix of the flexible manipulator while the vibration characteristics are determined by structural properties of the links such as the damping and stiffness parameters. Moreover, in contrast to the dynamic model of rigid-link robots the dynamic model of flexible-link robots is an infinite dimensional one. As in the case of the rigid-link manipulators there is a certain number of mechanical degrees of freedom associated to the rotational motion of the robot's joints and there is also an infinite number of degrees of freedom associated to the vibration modes in which the deformation of the flexible link is decomposed The controller of a flexible manipulator must achieve the same motion objectives as in the case of a rigid manipulator, i.e. tracking of specific joints position and velocity setpoints. Additionally, it must also stabilize and asymptotically eliminate the vibrations of the flexible-links that are naturally excited by the joints' rotational motion. A first approach for the control of flexible-link robots is to consider the vibration modes as additional state variables and to develop stabilizing feedback controller for the extended state-space model of the flexible manipulator. To this end, one can use again (i) control based on global linearization methods, (ii) control based on approximate linearization methods, (iii) control based on Lyapunov methods. Another approach to the solution of the control problem of flexible manipulators is to treat the robot as a distributed parameter system and to apply control directly to the partial differential equations models that describe the motion of the flexible links. Again global asymptotic stability for this control approach can be demonstrated. On the other side, nonlinear filtering methods can be used for implementing state estimation-based feedback control through the measurement of a limited number of elements from the flexible robot's state vector. In particular, the topics which are developed by the present chapter are as follows: (a) Inverse dynamics control of flexible-link robotic manipulators (b) sliding-mode control of flexible-link robotic manipulators.

G. Rigatos and K. Busawon, *Robotic Manipulators and Vehicles*,
Studies in Systems, Decision and Control 152,
https://doi.org/10.1007/978-3-319-77851-8_5

5.1 Chapter Overview

The topics which are developed by the present chapter are as follows: (a) Inverse dynamics control of flexible-link robotic manipulators (b) sliding-mode control of flexible-link robotic manipulators.

With reference to (a) a comparative study on representative methods for model-based and model-free control of flexible-link robots is given. Model-based techniques for the control of flexible-link robots such as inverse dynamics control can come up against limitations when an accurate model is unavailable, due to parameters uncertainty or truncation of high order vibration modes. On the other hand, model-free control methods, such as energy-based control can result in stabilization and satisfactory trajectory tracking performance of flexible-link robots.

With reference to (b) a robust control approach for a 2-link flexible robotic manipulator is developed that comprises sliding-mode control theory and Kalman Filtering. It is aimed to achieve: (i) simultaneous position control and suppression of the flexible structure vibrations. Assuming a known model of the robot dynamics, this can be achieved with the use of robust model-based control schemes, such as sliding-mode control, (ii) estimation of the complete state vector of the vibrating structure, so as to implement state-feedback control. To solve the latter problem, in this chapter, state estimation for the flexible-link robot is implemented with the use of Kalman Filtering. The fast recursion of the Kalman Filter provides real-time estimates of the robot's state vector through the processing of measurements coming from a limited number of sensors.

5.2 Inverse Dynamics Control of Flexible-Link Robots

5.2.1 Outline

Flexible-link robots comprise an important class of systems that include lightweight arms for assembly, civil infrastructure, bridge/vehicle systems, military applications and large-scale space structures. Modelling and vibration control of flexible systems have received a great deal of attention in recent years [224, 231, 442]. This section presents a comparative study on representative methods for model-based and model-free control of flexible-link robots. Conventional approaches to design a control system for a flexible-link robot often involve the development of a mathematical model describing the robot dynamics, and the application of analytical techniques to this model to derive an appropriate control law [22, 75, 119]. Usually, such a mathematical model consists of nonlinear partial differential equations, most of which are obtained using some approximation or simplification [224, 442]. The inverse dynamics model-based control for flexible link robots relies on modal analysis, i.e. on the assumption that the deformation of the flexible link can be written as a finite series expansion containing the elementary vibration modes [583]. However, this

inverse-dynamics model-based control may result into unsatisfactory performance when an accurate model is unavailable, due to parameters uncertainty or truncation of high order vibration modes [268].

Another model-based approach for the control of flexible-link robots is flatness-based control. Flatness-based control is a powerful tool for the control of distributed parameter systems which does not follow modal analysis but the description of the flexible robot using the concept of *differential flatness* [16, 39, 146]. It has been shown that flexible-link robots and flexible beams are flat systems and thus flatness-based control can be efficiently used for trajectory tracking of flexible-link manipulators [145, 337, 349, 476]. The decomposition of the desirable trajectory into a series of a reference flat output (Gevrey function) and its derivatives enables to generate open-loop control that assures tracking of the desirable trajectory. To achieve additional robustness a PID control loop can be designed to operate in parallel to the flatness-based controller of the flexible-link manipulator. Different model-based approaches for the control of flexible link manipulators have been also developed. In [365] wave-based control of flexible-link robots has been proposed. First a new wave-based model of uniform mass-spring systems was introduced and next this model was used to derive a control method for flexible-link robotic systems. In [41], a survey of model-based approaches for the control of flexible-link manipulators has been given.

To overcome the inefficiencies of the aforementioned inverse-dynamics control, model-free control methods have been studied [351, 529, 612]. A number of research papers employ model-free approaches for the control of flexible-link robots based on fuzzy logic and neural networks. In [557] control of a flexible manipulator with the use of a neuro-fuzzy method is described, where the weighting factor of the fuzzy logic controller is adjusted by the dynamic recurrent identification network. The controller works without any prior knowledge about the manipulator's dynamics. Control of the end-effector's position of a flexible-link manipulator with the use of a neural and a fuzzy controller has been presented in [531, 543, 575]. In [575] an intelligent optimal control for a nonlinear flexible robot arm driven by a permanent-magnet synchronous servo motor has been designed using a fuzzy neural network control approach. This consists of an optimal controller which minimizes a quadratic performance index and a fuzzy neural-network controller that learns the uncertain dynamics of the flexible manipulator. In [543] a fuzzy controller has been developed for a three-link robot with two rigid links and one flexible fore-arm. This controller's design is based on fuzzy Lyapunov synthesis where a Lyapunov candidate function has been chosen to derive the fuzzy rules. In [530] a neuro-fuzzy scheme has been proposed for position control of the end effector of a single-link flexible robot manipulator. The scale factors of the neuro-fuzzy controller are adapted on-line using a neural network which is trained with an improved back-propagation algorithm. In [73] two different neuro-fuzzy feed-forward controllers have been proposed to compensate for the nonlinearities of a flexible manipulator. In [412] the dynamics of a flexible link has been modeled using modal analysis and then an inverse dynamics fuzzy controller has been employed to obtain tracking and deflection control. In [503] a fuzzy logic controller has been applied to a flexible-link manipulator. In this distributed fuzzy logic controller the two velocity variables which have higher

importance have been grouped together as the inputs to a velocity fuzzy controller while the two displacement variables which have lower importance degrees have been used as inputs to a displacement fuzzy logic controller. In [204] adaptive control for a flexible-link manipulator has been achieved using a neuro-fuzzy time-delay controller. In [362] a genetic algorithm has been used to improve the performance of a fuzzy controller designed to compensate for the links' flexibility and the joints' flexibility of a robotic manipulator.

In this section the energy-based model-free control method of flexible-link robots is examined and shown to be equally effective to the model-based control methods. In the energy-based control method, instead of using the dynamical model of the links, the main stability results are derived with the use of the total energy and the energy-work relationship of the whole system [164, 491].

5.2.2 *Model-Based Control of Flexible Link Robots*

5.2.2.1 The Inverse Dynamics Control Method

A common approach in modelling of flexible-link robots is depends on the Euler-Bernoulli model [583]. This model consists of nonlinear partial differential equations, which are obtained using some approximation or simplification. In case of a single-link flexible manipulator the basic variables of this model are $w(x,t)$ which is the deformation of the flexible link, and $\theta(t)$ which is the joint's angle.

$$E \cdot I \cdot w''''(x,t) + \rho \ddot{w}(x,t) + \rho x \ddot{\theta}(t) = 0 \tag{5.1}$$

$$I_t \ddot{\theta}(t) + \rho \int_0^L x \ddot{w}(x,t) dx = T(t) \tag{5.2}$$

In Eqs. (5.1) and (5.2), $w''''(x,t) = \frac{\partial^4 w(x,t)}{\partial x^4}$,$\ddot{w}(x,t) = \frac{\partial^2 w(x,t)}{\partial t^2}$, while I_t is the moment of inertia of a rigid link of length L, ρ denotes the uniform mass density and EI is the uniform flexural rigidity with units $N \cdot m^2$. To calculate $w(x,t)$, instead of solving analytically the above partial differential equations, modal analysis can be used which assumes that $w(x,t)$ can be approximated by a weighted sum of orthogonal basis functions

$$w(x,t) = \sum_{i=1}^{n_e} \phi_i(x) v_i(t) \tag{5.3}$$

where index $i = [1, 2, \ldots, n_e]$ denotes the normal modes of vibration of the flexible link. Using modal analysis a dynamical model of finite-dimensions is derived for the flexible link robot. Without loss of generality assume a 2-link flexible robot (Fig. 5.1) and that only the first two vibration modes of each link are significant ($n_e = 2$). Σ_1 is a point on the first link with reference to which the deformation vector is measured.

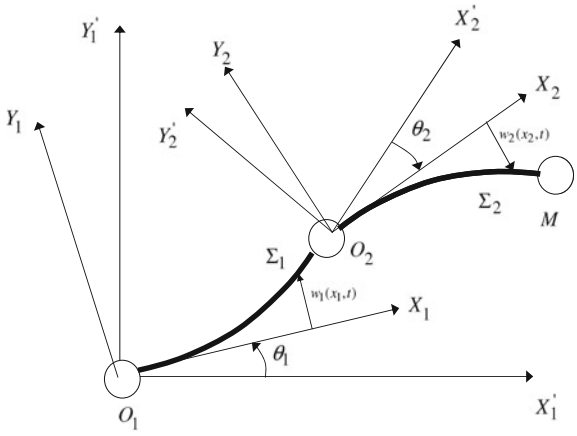

Fig. 5.1 A 2-DOF flexible-link robot

Similarly, Σ_2 is a point on the second link with reference to which the associated deformation vector is measured. In that case the dynamic model of the robot becomes [268, 583]:

$$\begin{pmatrix} M_{11}(z) & M_{12}(z) \\ M_{21}(z) & M_{22}(z) \end{pmatrix} \cdot \begin{pmatrix} \ddot{\theta} \\ \ddot{v} \end{pmatrix} + \begin{pmatrix} F_1(z,\dot{z}) \\ F_2(z,\dot{z}) \end{pmatrix} + \begin{pmatrix} 0_{2\times 2} & 0_{2\times 4} \\ 0_{4\times 2} & D(z) \end{pmatrix} \cdot \begin{pmatrix} \dot{\theta} \\ \dot{v} \end{pmatrix} + \\ + \begin{pmatrix} 0_{2\times 2} & 0_{2\times 4} \\ 0_{4\times 2} & K(z) \end{pmatrix} \cdot \begin{pmatrix} \theta \\ v \end{pmatrix} = \begin{pmatrix} T(t) \\ 0_{4\times 1} \end{pmatrix} \tag{5.4}$$

where $z = [\theta, v]^T$, with $\theta = [\theta_1, \theta_2]^T$, $v = [v_{11}, v_{12}, v_{21}, v_{22}]^T$ (vector of the vibration modes for links 1 and 2), and $[F_1(z,\dot{z}), F_2(z,\dot{z})]^T = [0,0]^T$ (centrifugal and Coriolis forces). The elements of the inertia matrix are: $M_{11} \in R^{2\times 2}$, $M_{12} \in R^{2\times 4}$, $M_{21} \in R^{4\times 2}$, $M_{22} \in R^{4\times 4}$. The damping and elasticity matrices of the aforementioned model are $D \in R^{4\times 4}$ and $K \in R^{4\times 4}$. Moreover the vector of the control torques is $T(t) = [T_1(t), T_2(t)]^T$.

The principle of inverse dynamics control is to transform the nonlinear system of Eq. (5.4) into a linear one, so that linear control techniques can be applied. From Eq. (5.4) it holds that:

$$M_{11}\ddot{\theta} + M_{12}\ddot{v} + F_1(z,\dot{z}) = T(t) \tag{5.5}$$

$$M_{21}\ddot{\theta} + M_{22}\ddot{v} + F_2(z,\dot{z}) + D\dot{v} + Kv = 0 \tag{5.6}$$

Equation (5.6) is solved with respect to $\ddot{v}$

$$\ddot{v} = -M_{22}^{-1}M_{21}\ddot{\theta} - M_{22}^{-1}F_2(z,\dot{z}) - M_{22}^{-1}D\dot{v} - M_{22}^{-1}Kv \tag{5.7}$$

Equation (5.7) is substituted in Eq. (5.5) which results into:

$$(M_{11} - M_{12}M_{22}^{-1}M_{21})\ddot{\theta} - M_{12}M_{22}^{-1}F_2(z,\dot{z}) - M_{12}M_{22}^{-1}D\dot{v} - M_{12}M_{22}^{-1}Kv + F_1(z,\dot{z}) = T(t) \tag{5.8}$$

The following control law is now introduced [583]:

$$T(t) = -M_{12}M_{22}^{-1}F_2(z,\dot{z}) - M_{12}M_{22}^{-1}D\dot{v} - \\ -M_{12}M_{22}^{-1}Kv + F_1(z,\dot{z}) + (M_{11} - M_{12}M_{22}^{-1}M_{21})u_0 \tag{5.9}$$

$$u_0 = \ddot{\theta}_d - K_d(\dot{\theta} - \dot{\theta}_d) - K_p(\theta - \theta_d) \tag{5.10}$$

By replacing Eqs. (5.9) in (5.8) one gets

$$(M_{11} - M_{12}M_{22}^{-1}M_{21})\ddot{\theta} - M_{12}M_{22}^{-1}F_2(z,\dot{z}) - M_{12}M_{22}^{-1}D\dot{v} - M_{12}M_{22}^{-1}Kv + F_1(z,\dot{z}) = \\ = -M_{12}M_{22}^{-1}F_2(z,\dot{z}) - M_{12}M_{22}^{-1}D\dot{v} - M_{12}M_{22}^{-1}Kv + F_1(z,\dot{z}) + (M_{11} - M_{12}M_{22}^{-1}M_{21})u_0$$

which finally results into

$$\ddot{\theta} = u_0 \tag{5.11}$$

Equation (5.11) implies that linearisation and decoupling of the robotic model has been achieved. Substituting Eqs. (5.10) into (5.11) gives:

$$\ddot{\theta} - \ddot{\theta}_d + K_d(\dot{\theta} - \dot{\theta}_d) + K_p(\theta - \theta_d) = 0 \Rightarrow \\ \ddot{e}(t) + K_d\dot{e}(t) + K_p e(t) = 0 \tag{5.12}$$

Gain matrices K_p and K_d are selected, so as to assure that the poles of Eq. (5.12) are in the left semiplane. This results into

$$lim_{t\to\infty}e(t) = 0 \Rightarrow lim_{t\to\infty}\theta(t) = \theta_d(t) \tag{5.13}$$

Consequently, for $\theta_d(t)$ =constant it holds $lim_{t\to\infty}\ddot{\theta}(t) = 0$. Then Eq. (5.7) gives

$$\ddot{v} = -M_{22}^{-1}F_2 - M_{22}^{-1}D\dot{v} - M_{22}^{-1}Kv \tag{5.14}$$

and for $F_2(z,\dot{z}) = 0$ results into

$$\ddot{v} + M_{22}^{-1}D\dot{v} + M_{22}^{-1}Kv = 0 \tag{5.15}$$

which is the differential equation of the free damped oscillator. Suitable selection of the damping matrix D and the elasticity matrix K assures that

$$lim_{t\to\infty}v(t) = 0 \tag{5.16}$$

5.2.2.2 Shortfalls of Inverse Dynamics Control for Flexible-Link Robots

The objective of the inverse-dynamics model-based control for flexible-link robots, that was presented in Sect. 5.2.2.1, is to force the rigid-mode variable $\theta(t)$ to follow

a desired trajectory or to converge to a certain set-point and at the same time to suppress the flexible modes of the links $v(t)$. However, this control approach appears several weaknesses [268]:
1. In general there are n_r flexible links, thus $\theta(t) \in R^{n_r}$. The control input available is $T(t) \in R^{n_r}$, since there is one actuator per link. Considering n_f flexible modes for each link means that $n_r \times n_f$ additional degrees of freedom are introduced. Thus appropriate control is required to suppress the vibrations. However, the number of control inputs is n_r which is less than the number of the degrees of freedom. Consequently, there is reduced control effectiveness.
2. The situation becomes more complicated, because by selecting the control input $T(t)$ to achieve practical tracking performance of the rigid variable $\theta(t)$, one actually destabilizes the flexible modes $v(t)$. This is due to the non-minimum phase nature of the zeros dynamics of the flexible-link arms.
3. Another drawback of model-based control is that the model of Eq. (5.4), is derived assuming a finite number of vibration modes. This simplification is not always applicable since higher-order modes may be excited. The proposed model-based control does not provide robustness to external disturbances.

5.2.3 Energy-Based Control of Flexible Link Robots

5.2.3.1 Energy-Based Control

To overcome the weaknesses of the inverse-dynamics model-based control for flexible link robots, model-free control methods have been proposed. Of interest is the energy-based control which requires only knowledge of the potential and kinetic energy of the flexible manipulator. Energy-based control of flexible-link robots assures closed-loop system stability in the case of constant set-points (point-to-point control).

The kinetic energy E_{kin} of a n-link flexible robot is given by [164, 583]

$$E_{kin} = \sum_{i=1}^{n} \frac{1}{2} \rho \int_0^{L_i} [\dot{p}_{x_i}^2 + \dot{p}_{y_i}^2] dx \tag{5.17}$$

In Eq. (5.17), p_{x_i} is the position of elementary segment of the ith link along x-axis, while p_{y_i} is the position of elementary segment of the ith link along y-axis. On the other hand the potential energy E_p of a planar n-link flexible robot is due to the links deformation and is given by

$$E_p = \sum_{i=1}^{n} \frac{1}{2} E I \int_0^{L_i} [\frac{\partial^2}{\partial x^2} w_i(x,t)]^2 dx \tag{5.18}$$

Thus to estimate the robot's potential energy, measurement of the flexible links strain $\frac{\partial^2 w_i(x,t)}{\partial x^2}$ is needed. The potential energy includes only the energy due to strain,

while the gravitational effect as well as longitudinal and torsional deformations are neglected.

Moreover, the energy provided to the flexible-link robot by the ith motor is given by

$$W_i = \int_0^t T_i(\tau)\dot{\theta}(\tau)d\tau \tag{5.19}$$

Consequently, the power of the ith motor is

$$P_i(t) = T_i(t)\dot{\theta}_i(t) \tag{5.20}$$

where $T_i(t)$ is the torque of the ith motor and $\dot{\theta}_i(t)$ is the motor's angular velocity. Thus, the aggregate motors energy is given by

$$W = \sum_{i=1}^{n}\int_0^t T_i(\tau)\dot{\theta}_i(\tau)d\tau \tag{5.21}$$

The energy that is provided to the flexible-link robot by its motors takes the form of: (i) potential energy (due to the deformation of the flexible links) and (ii) kinetic energy. This energy flow is described by

$$[E_{kin}(t) + E_p(t)] - [E_{kin}(0) + E_p(0)] = W \tag{5.22}$$

Energy-based control of flexible-link robots considers that the torque of the ith motor (control output) is based on a PD-type controller and is given by [164, 583]:

$$\begin{gathered} T_i(t) = -K_{p_i}[\theta_i(t) - \theta_{d_i}(t)] - K_{d_i}\dot{\theta}_i(t) - \\ -K_i w_i''(x,t)\int_0^t \dot{\theta}_i(s)w_i''(x,s)ds,\ i = 1,2,\ldots,n \end{gathered} \tag{5.23}$$

where K_{p_i} is the ith P control gain, K_{d_i} is the ith D control gain, θ_{d_i}, is the desirable angle of the ith link, K_i is also a positive (constant) gain, and $w_i(x,t)$ is the deformation of the ith link.

5.2.3.2 Stability Proof

The proposed control law of Eq. (5.23) assures the asymptotic stability of the closed-loop system in case of constant set-points (point to point control). The following Lyapunov (energy) function is considered [164, 583]:

$$V = E_{kin} + E_p + \frac{1}{2}\sum_{i=1}^{N} K_{p_i}[\theta_i(t) - \theta_{d_i}(t)]^2 + \frac{1}{2}\sum_{i=1}^{n} K_i[\int_0^t \dot{\theta}_i(s)w_i''(s,t)ds]^2 \tag{5.24}$$

where E_{kin} is given by Eq. (5.17) and denotes the kinetic energy of the robot's links, while E_p is given by Eq. (5.18) and denotes the potential energy of the robot's links due to deformation.

It holds that $V(t) > 0$ since $E_{kin} > 0$, $E_p > 0$, $\frac{1}{2}\sum_{i=1}^{n} K_{p_i}[\theta_i(t) - \theta_{d_i}(t)]^2 > 0$ and $\frac{1}{2}\sum_{i=1}^{n} K_i[\int_0^t \dot{\theta}_i(t) w_i(s,t)]^2 > 0$. Moreover, it holds that

$$\begin{array}{c}\dot{V}(t) = \dot{E}_{kin} + \dot{E}_p + \sum_{i=1}^{n} K_{p_i}[\theta_i(t) - \theta_{d_i}(t)]\dot{\theta}_i(t) + \\ \frac{1}{2}\sum_{i=1}^{n} 2K_i[\int_0^t \dot{\theta}_i(s,t) w_i''(s,t) ds][\dot{\theta}_i(t) w_i''(x,t)]\end{array} \tag{5.25}$$

while using Eqs. (5.20) and (5.22) the derivative of the robot's energy is found to be

$$\dot{E}_{kin}(t) + \dot{E}_p(t) = \sum_{i=1}^{n} T_i(t)\dot{\theta}_i(t) \tag{5.26}$$

where the torque generated by the ith motor is given by Eq. (5.23). By substituting Eqs. (5.26) and (5.23) in (5.25) one gets

$$\begin{array}{c}\dot{V}(t) = -\sum_{i=1}^{n} K_{p_i}[\theta_i(t) - \theta_{d_i}(t)]\dot{\theta}_i(t) - \\ -\sum_{i=1}^{n} K_{d_i}\dot{\theta}_i^2(t) - \sum_{i=1}^{n}[K_i w_i''(x,t)\int_0^t \dot{\theta}_i(s) w_i''(s,t) ds]\dot{\theta}_i(t) \\ +\sum_{i=1}^{n} K_{p_i}[\theta_i(t) - \theta_{d_i}(t)]\dot{\theta}_i(t) + \sum_{i=1}^{n}[K_i w_i''(x,t)\int_0^t \dot{\theta}_i(s) w_i''(s,t) ds]\dot{\theta}_i(t)\end{array} \tag{5.27}$$

which finally results into,

$$\dot{V}(t) = -\sum_{i=1}^{n} K_{d_i}\dot{\theta}_i^2 \tag{5.28}$$

Obviously, from Eq. (5.28) it holds that $\dot{V}(t) \leq 0$, which implies stability of the closed-loop system, but not asymptotic stability. Asymptotic stability can be proven as follows [583]: If the ith link did not converge to the desirable angle, i.e. $lim_{t\to\infty}\theta_i(t) = a_i \neq \theta_{d_i}(t)$ then the torque of the ith motor would become equal to a small positive constant. This is easy to prove from Eq. (5.23) where the terms $K_{d_i}\dot{\theta}_i(t) = 0$, $K_i w_i(x,t)\int_0^t \dot{\theta}_i(s) w_i''(s,t) ds = 0$, while the term $K_{p_i}[\theta_i(t) - \theta_{d_i}(t)] = K_{p_i} a_i$ becomes equal to a positive constant.

However, if $T_i(t) = \text{constant} \neq 0$ then the ith link should continue to rotate. This means that $\theta_i(t) \neq a_i$, which contradicts the initial assumption $lim_{t\to\infty}\theta_i(t) = a_i$. Therefore, it must hold $lim_{t\to\infty} T_i(t) = 0$ and $lim_{t\to\infty}\theta_i(t) = \theta_{d_i}(t)$. Consequently, $lim_{t\to\infty} V(t) = 0$.

The proposed energy-based controller is a decentralized controller since the control signals $T_i(t)$ of the ith motor are calculated using only the angle $\theta_i(t)$ and the deformation $w_i(x,t)$ of the ith link.

5.2.4 Force Control in Flexible-Link Robots

Up to now the study of control methods for flexible-link robots followed the assumption that the robot operated in the free space. However, when in contact with a surface, forces are exerted to robot's end-effector and a significant issue that has to be taken into account in the design of the robotic controller is force control. To solve the force control problem, a kinematic model of a flexible-link robot is first introduced.

5.2.4.1 Overview of the Kinematic Model of Flexible-Link Robots

Assume the ith link of the flexible-link robot and the associated rotating frame $O_i X_i Y_i$ (Fig. 5.1). Then the vector of coordinates of the end-effector M is given by

$$p_M^i = [x_i, w_i(x_i)]^T \tag{5.29}$$

The coordinates of the end-effector in the inertial frame $O_1 X_1^{'} Y_1^{'}$ is given by

$$p_M = r_i + W_i p_M^i \tag{5.30}$$

with

$$\begin{gathered} W_i = W_{i-1} E_{i-1} R_i = \hat{W}_{i-1} R_i \\ \hat{W}_0 = I \end{gathered} \tag{5.31}$$

where R_i is the rigid rotation matrix that aligns the rotating frame of the ith link to the inertial frame of the same link, and E_{i-1} is the flexible rotation matrix that aligns the inertial frame of link i to the rotational frame of link $i-1$:

$$R_i = \begin{pmatrix} cos(\theta_i) & -sin(\theta_i) \\ sin(\theta_i) & cos(\theta_i) \end{pmatrix}, \quad E_i = \begin{pmatrix} 1 & -w_{ie}^{'} \\ w_{ie}^{'} & 1 \end{pmatrix} = \begin{pmatrix} 1 & -\frac{\partial w_i}{\partial x_i} \\ \frac{\partial w_i}{\partial x_i} & 1 \end{pmatrix} \tag{5.32}$$

$$r_i = r_{i-1} + W_i r_i^{i-1} \tag{5.33}$$

where r_i^{i-1} is the distance vector between the origin of the and ith and the $i-1$th frame, r_i is the distance vector between the origin of the ith rotational frame and the inertial frame, and W_i is the rotation matrix calculated with the use of Eq. (5.31).

Using Eqs. (5.33) and (5.43) in the 2-DOF flexible-link robot depicted in Fig. 5.1, one obtains

$$r_2 = r_1 + W_1 r_2^1 = \begin{pmatrix} L_1 cos(\theta_1) - w_1(L_1, t) sin(\theta_1) \\ L_1 sin(\theta_1) + w_1(L_1, t) cos(\theta_1) \end{pmatrix} \tag{5.34}$$

$$p_M = r_2 + W_2 p_M^2 \tag{5.35}$$

where

$$p_M^2 = \begin{pmatrix} L_2 \\ w_2(L_2, t) \end{pmatrix}, W_2 = R_1 E_1 R_2 = \\ \begin{pmatrix} cos(\theta_1) & -sin(\theta_1) \\ sin(\theta_1) & cos(\theta_1) \end{pmatrix} \cdot \begin{pmatrix} 1 & -w'_{1e} \\ w'_{1e} & 1 \end{pmatrix} \cdot \begin{pmatrix} cos(\theta_2) & -sin(\theta_2) \\ sin(\theta_2) & cos(\theta_2) \end{pmatrix} \tag{5.36}$$

The differential kinematic model of the flexible-link robot can now be calculated. The coordinates of the end-effector in the inertial frame are given by Eq. (5.30). According to modal analysis the deformation $w_i(x_i, t)$ in normal modes of vibration is given by Eq. (5.3). Using the previous 2 equations the kinematic model can be written as a function of the joint angles θ and of the normal modes of vibration v.

$$p = k(\theta, v) \tag{5.37}$$

The velocity of the end-effector is calculated through the differentiation of Eq. (5.43).

$$\dot{p}_M = \dot{r}_i + \dot{W}_i p_M^i + W_i \dot{p}_M^i \tag{5.38}$$

Moreover, it holds that $\dot{r}_{i+1}^i = \dot{p}_M^i(L_i) = [0, \dot{w}_i(x_i = L_i)]^T$ since there is no longitudinal deformation ($\dot{x}_i = 0$). It also holds that

$$\dot{W}_i = \dot{\hat{W}}_{i-1} R_i + \hat{W}_{i-1} \dot{R}_i \\ \dot{\hat{W}}_i = \dot{W}_i E_i + W_i \dot{E}_i \tag{5.39}$$

It also holds that

$$\dot{R}_i = S R_i \dot{\theta}_i \\ \dot{E}_i = S \dot{w}'_{ie} \tag{5.40}$$

with $S = \begin{pmatrix} 0 & -1 \\ 1 & 0 \end{pmatrix}$. Substituting Eqs. (5.39) and (5.40) in (5.38) the differential kinematic model of the flexible-link robot is obtained:

$$\dot{p} = J_\theta(\theta, v)\dot{\theta} + J_v(\theta, v)\dot{v} \tag{5.41}$$

where

$J_\theta = \frac{\partial k}{\partial \theta}$: is the Jacobian with respect to θ
$J_v = \frac{\partial k}{\partial v}$: is the Jacobian with respect to v.
If the end-effector is in contact with the surface $\Omega(\theta)$ and is subject to contact-forces $F = [F_x, F_y]$ then the torques which are developed to the joints are:
$J_\theta^T F$: torques that produce the work associated with the rotation angle θ.
$J_v^T F$: torques that produce work associated with the deformation modes v.

The dynamic model of the flexible-link robot given in Eq. (5.4) is corrected into:

$$\begin{pmatrix} M_{11}(z) & M_{12}(z) \\ M_{21}(z) & M_{22}(z) \end{pmatrix} \begin{pmatrix} \ddot{\theta} \\ \ddot{v} \end{pmatrix} + \begin{pmatrix} F_1(z,\dot{z}) \\ F_2(z,\dot{z}) \end{pmatrix} + \\ + \begin{pmatrix} 0_{2\times 2} & 0_{2\times 4} \\ 0_{4\times 2} & D(z) \end{pmatrix} \begin{pmatrix} \dot{\theta} \\ \dot{v} \end{pmatrix} + \begin{pmatrix} 0_{2\times 2} & 0_{2\times 4} \\ 0_{4\times 2} & K(z) \end{pmatrix} \begin{pmatrix} \theta \\ v \end{pmatrix} = \begin{pmatrix} T(t) - J_\theta^T(\theta, v)F \\ -J_v^T(\theta, v)F \end{pmatrix} \tag{5.42}$$

For a two-link flexible robot of Fig. 5.1 one gets

$$p_M = \begin{pmatrix} L_1 cos(\theta_1) - w_1(L_1, t) sin(\theta_1) \\ L_1 sin(\theta_1) + w_1(L_1, t) cos(\theta_1) \end{pmatrix} + \\ + \begin{pmatrix} cos(\theta_1+\theta_2) - w_{1e}^{'} sin(\theta_1+\theta_2) & -sin(\theta_1+\theta_2) - w_{1e}^{'} cos(\theta_1+\theta_2) \\ sin(\theta_1+\theta_2) + w_{1e}^{'} cos(\theta_1+\theta_2) & cos(\theta_1+\theta_2) - w_{1e}^{'} sin(\theta_1+\theta_2) \end{pmatrix} \begin{pmatrix} L_2 \\ w_2 \end{pmatrix} \tag{5.43}$$

with

$$\begin{aligned} w_1(L_1, t) &= \phi_{11}(L_1) v_{11}(t) + \phi_{12}(L_1) v_{12}(t) \\ w_2(L_2, t) &= \phi_{21}(L_2) v_{21}(t) + \phi_{22}(L_2) v_{22}(t) \\ w_{1e}^{'} &= \frac{\partial w_1(x,t)}{\partial x}|_{x=L_1} = \phi_{11}^{'}(L_1) v_{11}(t) + \phi_{12}^{'}(L_1) v_{12}(t) \end{aligned} \tag{5.44}$$

The Jacobian J_θ is

$$J_\theta = \begin{pmatrix} \frac{\partial p_M^{(1)}}{\partial \theta_1} & \frac{\partial p_M^{(1)}}{\partial \theta_2} \\ \frac{\partial p_M^{(2)}}{\partial \theta_1} & \frac{\partial p_M^{(2)}}{\partial \theta_2} \end{pmatrix} \tag{5.45}$$

$$\frac{\partial p_M^{(1)}}{\partial \theta_1} = -L_1 sin(\theta_1) - w_1(L_1, t) cos(\theta_1) - L_2 sin(\theta_1+\theta_2) - \\ -L_2 w_{1e}^{'} cos(\theta_1+\theta_2) - w_2(L_2, t) cos(\theta_1+\theta_2) + w_2(L_2, t) w_{1e}^{'} sin(\theta_1+\theta_2)$$

$$\frac{\partial p_M^{(2)}}{\partial \theta_1} = L_1 cos(\theta_1) - w_1(L_1, t) sin(\theta_1) + L_2 cos(\theta_1+\theta_2) - L_2 w_{1e}^{'} sin(\theta_1+\theta_2) - \\ -w_2(L_2, t) sin(\theta_1+\theta_2) + w_2(L_2, t) w_{1e}^{'} cos(\theta_1+\theta_2)$$

$$\frac{\partial p_M^{(1)}}{\partial \theta_2} = -L_2 sin(\theta_1+\theta_2) - L_2 w_{1e}^{'} cos(\theta_1+\theta_2) - w_2(L_2, t) cos(\theta_1+\theta_2) + \\ +w_2(L_2, t) w_{1e}^{'} sin(\theta_1+\theta_2)$$

$$\frac{\partial p_M^{(2)}}{\partial \theta_2} = L_2 cos(\theta_1+\theta_2) - L_2 w_{1e}^{'} sin(\theta_1+\theta_2) - w_2(L_2, t) sin(\theta_1+\theta_2) - \\ -w_2(L_2, t) w_{1e}^{'} cos(\theta_1+\theta_2)$$

Similarly, the Jacobian J_v is calculated:

$$J_v = \begin{pmatrix} \frac{\partial p_M^{(1)}}{\partial v_{11}} & \frac{\partial p_M^{(1)}}{\partial v_{12}} & \frac{\partial p_M^{(1)}}{\partial v_{21}} & \frac{\partial p_M^{(1)}}{\partial v_{22}} \\ \frac{\partial p_M^{(2)}}{\partial v_{11}} & \frac{\partial p_M^{(2)}}{\partial v_{12}} & \frac{\partial p_M^{(2)}}{\partial v_{21}} & \frac{\partial p_M^{(2)}}{\partial v_{22}} \end{pmatrix} \tag{5.46}$$

$$\frac{\partial p_M^{(1)}}{\partial v_{11}} = -\phi_{11}(L_1) sin(\theta_1) - L_2 \phi_{11}^{'}(L_1) sin(\theta_1+\theta_2) - w_2(L_2, t) \phi_{11}^{'}(L_1) cos(\theta_1+\theta_2)$$

$$\frac{\partial p_M^{(1)}}{\partial v_{12}} = -\phi_{12}(L_1)sin(\theta_1) - L_2\phi_{12}^{'}(L_1)sin(\theta_1+\theta_2) - w_2(L_2,t)\phi_{12}^{'}(L_1)cos(\theta_1+\theta_2)$$

$$\frac{\partial p_M^{(1)}}{\partial v_{21}} = -\phi_{21}(L_2)sin(\theta_1+\theta_2) - \phi_{21}(L_2)w_{1e}^{'}cos(\theta_1+\theta_2)$$

$$\frac{\partial p_M^{(1)}}{\partial v_{22}} = -\phi_{22}(L_2)sin(\theta_1+\theta_2) - \phi_{22}(L_2)w_{1e}^{'}cos(\theta_1+\theta_2)$$

$$\frac{\partial p_M^{(2)}}{\partial v_{11}} = \phi_{11}(L_1)cos(\theta_1) + L_2\phi_{11}^{'}(L_1)cos(\theta_1+\theta_2) - w_2(L_2,t)\phi_{11}^{'}(L_1)sin(\theta_1+\theta_2)$$

$$\frac{\partial p_M^{(2)}}{\partial v_{12}} = \phi_{12}(L_1)cos(\theta_1) + L_2\phi_{12}^{'}(L_1)cos(\theta_1+\theta_2) - w_2(L_2,t)\phi_{12}^{'}(L_1)sin(\theta_1+\theta_2)$$

$$\frac{\partial p_M^{(2)}}{\partial v_{21}} = \phi_{21}(L_2)cos(\theta_1+\theta_2) - \phi_{21}(L_2)w_{1e}^{'}sin(\theta_1+\theta_2)$$

$$\frac{\partial p_M^{(2)}}{\partial v_{22}} = \phi_{22}(L_2)cos(\theta_1+\theta_2) - \phi_{22}(L_2)w_{1e}^{'}sin(\theta_1+\theta_2)$$

5.2.4.2 Interaction with the Compliant Surface

A simple model of elastic force due to contact of the end-effector with a surface is given by:

$$F = K_e\eta\eta^T(p - p_e) \tag{5.47}$$

where $p = k(\theta, v)$ are the coordinates of the end-effector which are calculated from the kinematic model, and η is a vector normal to the surface p_e. From the second line of the dynamic model of Eq. (5.42) one obtains:

$$M_{21}\ddot{\theta} + M_{22}\ddot{v} + D\dot{v} + Kv = -J_v^T(\theta, v)F \tag{5.48}$$

In the steady-state one obtains

$$\begin{gathered} v = -K^{-1}J_v^T(\theta,v)F - K^{-1}J_v^T(\theta,v)\eta K_e(p_n - p_{en}) \Rightarrow \\ v = -K^{-1}J_{vn}K_e(p_n - p_{en}) \end{gathered} \tag{5.49}$$

where $p_n = \eta^T p$, $p_{e_n} = \eta^T p_e$, and $J_{v_n} = J_v^T\eta$. The derivative of Eq. (5.49) with respect to t is calculated.

$$\begin{gathered} \dot{v} = \frac{\partial v}{\partial\theta}\frac{\partial\theta}{\partial t} = \frac{\partial}{\partial\theta}\{-K^{-1}J_{v_n}K_e(p_n - p_{en})\}\dot{\theta} \Rightarrow \\ \dot{v} = -K^{-1}\frac{\partial J_{v_n}}{\partial\theta}K_e(p_n - p_{en}) + K^{-1}J_{v_n}K_e\frac{\partial p_{e_n}}{\partial\theta}\dot{\theta} \end{gathered} \tag{5.50}$$

which finally results into

$$\dot{v} = -K^{-1}K_eJ_f(\theta)\dot{\theta} \tag{5.51}$$

with $J_f(\theta) = \frac{\partial J_{v_n}}{\partial\theta}K_e(p_n - p_{en}) + K^{-1}J_{v_n}K_e\frac{\partial p_{e_n}}{\partial\theta}$. Substituting Eq. (5.51) into (5.41) gives:

$$\begin{gathered}\dot{p} = J_\theta(\theta, v)\dot{\theta} + J_v(\theta, v)\{-K^{-1}K_e J_f(\theta)\} \Rightarrow \\ \dot{p} = \{J_\theta(\theta, v) - K^{-1}K_e J_v(\theta, v) J_f(\theta)\}\end{gathered} \tag{5.52}$$

The overall Jacobian matrix J_p is defined as:

$$J_p = J_\theta(\theta, v) - K^{-1}K_e J_v(\theta, v) J_f(\theta) \tag{5.53}$$

which relates the velocity of the end-effector with the angular velocity of the joints

$$\dot{p} = J_p(\theta, v)\dot{\theta} \tag{5.54}$$

5.2.4.3 Force Control

The desirable contact force along the normal vector of surface p_e is denoted as F_d and corresponds to the desirable position p_d. The relation between F_d and p_d is given by

$$p_{d_n} = \eta^T p_d = K_e^{-1} F_d + p_{e_n} \tag{5.55}$$

or equivalently $p_{d_n} - p_{e_n} = K_e^{-1} F_d \Rightarrow \eta^T p_d - \eta^T p_e = K_e^{-1} F_d$. Thus to succeed contact force equal to F_d the end-effector should reach the depth $\eta^T p_d - \eta^T p_e$. The design of the force controller comprises the following steps [509]:
1. For a certain force set-point F_d the corresponding position of the end-effector is calculated using Eq. (5.55).
2. Knowing p_d an inverse kinematics algorithm is used to calculate the associated joint angles θ_d and the vibration modes v_d.
3. The values of θ_d and v_d are used as set-points of a simple proportional-derivative joint controller, as the ones described in the previous sections.
The inverse kinematics problem can be solved with the use of an inverse kinematics algorithm which enables the calculation of θ_d and v_d through the following relation:

$$\dot{\theta} = J_P^T(\theta, v) K_p (p_d - p) \tag{5.56}$$

where J_p is the Jacobian of Eq. (5.53), p is the current position of the end-effector, p_d is the desirable position of the end-effector, and K_p is the diagonal feedback matrix of Eq. (5.56). The convergence conditions of the inverse kinenatics algorithm have been studied [509]. The calculated values θ_d and v_d which are associated with the desirable position p_d are introduced as set-points in the PD controller of each link. This is given in:

$$T(t) = K_1(\theta_d - \theta) + K_2\dot{\theta} + J_\theta^T(\theta_d, v_d) F_d n \tag{5.57}$$

where $F_d n = K_e[\eta^T p_d - \eta^T p_e]\eta$ and J_θ is the Jacobian of Eq. (5.45). The term $J_\theta^T F_d n$ is added to the control signal to compensate for the torques which are induced to the joints due to the contact forces.

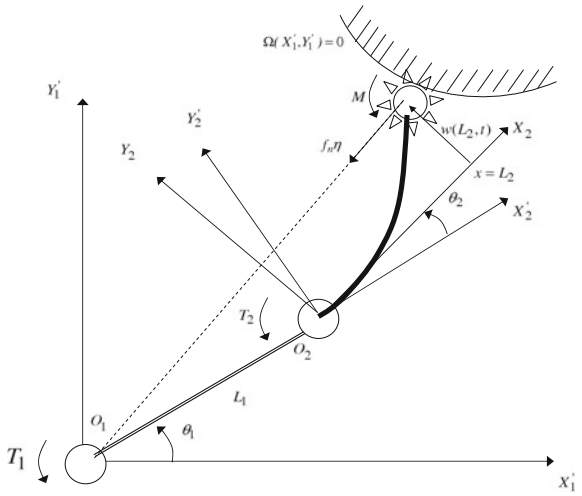

Fig. 5.2 A flexible-link robot which operates in the presence of compliance forces

The discrete-time solution of the inverse kinematics gives

$$\theta_d(k+1) = \theta_d(k) + T_s J_P^T(\theta_d(k), v_d(k)) K_p[p_d(k) - p(k)] \tag{5.58}$$

where the Jacobian J_p is given by Eq. (5.53), and T_s is the sampling period. From Eq. (5.51), one obtains iteratively the setpoints for the normal vibration modes,

$$v_d(k+1) = -K^{-1} K_e J_{v_n}(\theta_d(k))[p_n(k) - p_{e_n}(k)] \tag{5.59}$$

with $p_n = \eta^T p$, $p_{e_n} = \eta^T p_e$ and $J_{v_n} = J_v^T \eta$ (Fig. 5.2).

5.2.5 *Simulation Results*

The performance of the previously analyzed model-free control method (energy-based control) is compared to the performance of model-based techniques (inverse-dynamics control), in a simulation case study for planar 2-DOF manipulators (Fig. 5.2).

5.2.5.1 Model-Based Control of Flexible-Link Robots

The 2-DOF flexible link robot of Fig. 5.1 is considered. The robot is planar and consists of two flexible links of length $L_1 = 0.45\,\text{m}$ and $L_2 = 0.45\,\text{m}$, respectively. The dynamic model of the robot is given by Eq. (5.4). The elements of the inertia matrix M are:

$$M_{11} = \begin{pmatrix} 1 & 2 \\ 2 & 1 \end{pmatrix},\ M_{12} = M_{21}^T = \begin{pmatrix} 1 & 1 & 0.2 & 0.3 \\ 0.5 & 0.1 & 2 & 0.7 \end{pmatrix},\ M_{22} = \begin{pmatrix} 1 & 0 \\ 0 & 1 \end{pmatrix}$$

The damping matrix was taken to be $D = diag\{0.04, 0.08, 0.03, 0.06\}$ while the stiffness matrices was selected as $K = diag\{0.02, 0.04, 0.03, 0.06\}$. The inverse dynamics control law given in Eqs. (5.9) and (5.10) is employed. The selection of the gain matrices K_p and K_d determines the transient response of the closed loop system. The following controller gains have been considered: $K_p = diag\{0.2, 0.2\}$ and $K_d = diag\{0.1, 0.1\}$. The desirable joints positions are $\theta_{d_1} = 1$ rad and $\theta_{d_2} = 1.4$ rad. The performance of the model-based controller is given in Fig. 5.3.

Moreover, it is considered that an additive disturbance torque appears on each joint. The disturbance is given by $d_i(t) = 0.3cos(t)$. The performance of the model-based controller of the flexible-link robot in the presence of disturbance is depicted in Fig. 5.4. It can be seen that vibrations around the desirable joint positions cannot be eliminated.

5.2.5.2 Energy-Based Control

The same robotic model as in Sect. 5.3.4.1 is used to simulate the variation of the manipulator's joints with respect to time. Energy-based control of flexible-link robots is based on Eq. (5.23). The following controller gains have been used: $K_p = diag\{1.9, 5.6\}$, $K_d = diag\{7.2, 23.3\}$ and $K_i = diag\{0.1, 0.1\}$. The desirable joint positions are again $\theta_{d_1} = 1.0$ rad and $\theta_{d_2} = 1.4$ rad. To derive the control signal of Eq. (5.23) the strains at the base of each link were used, i.e. $w_i''(0, t)$. The performance of the energy-based controller in the case of the 2-DOF flexible link robot is shown in Fig. 5.5.

Moreover, the performance of the energy-based controller in presence of the external disturbances of Sect. 5.3.4.1 is given in Fig. 5.6. Suppression of the vibrations can be achieved if the elements of the gain matrix K_d are given higher values.

5.3 Sliding-Mode Control of Flexible-Link Manipulators

5.3.1 Outline

In the previous sections it has been pointed out that the control for flexible-link robots is a non-trivial problem that has elevated difficulty comparing to the control of rigid-link manipulators [450, 583]. This is because the dynamic model of the flexible-link robot contains the nonlinear rigid link motion coupled with the distributed effects of the links' flexibility. This coupling depends on the inertia matrix of the flexible manipulator while the vibration characteristics are determined by structural properties of the links such as the damping and stiffness parameters. Moreover, in contrast

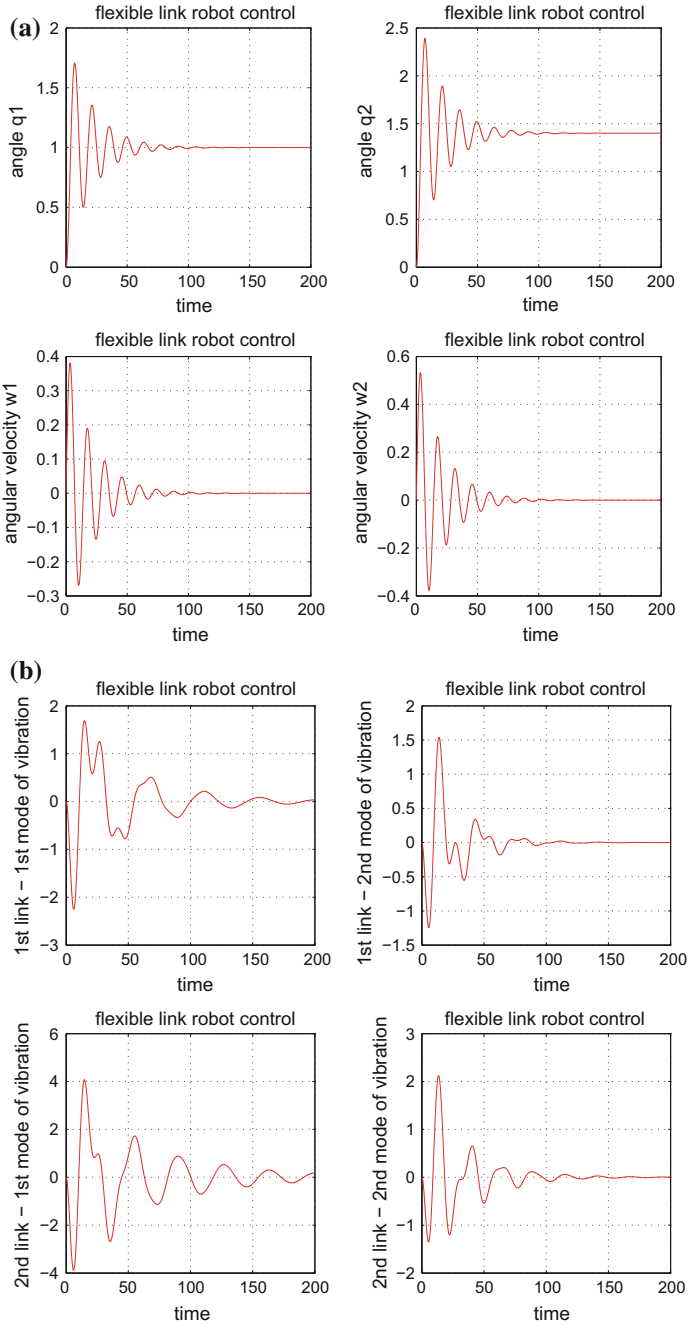

Fig. 5.3 Model-based control of a 2-link flexible robot **a** joints' angles and joints' angular velocity, **b** the first two vibration modes for each link

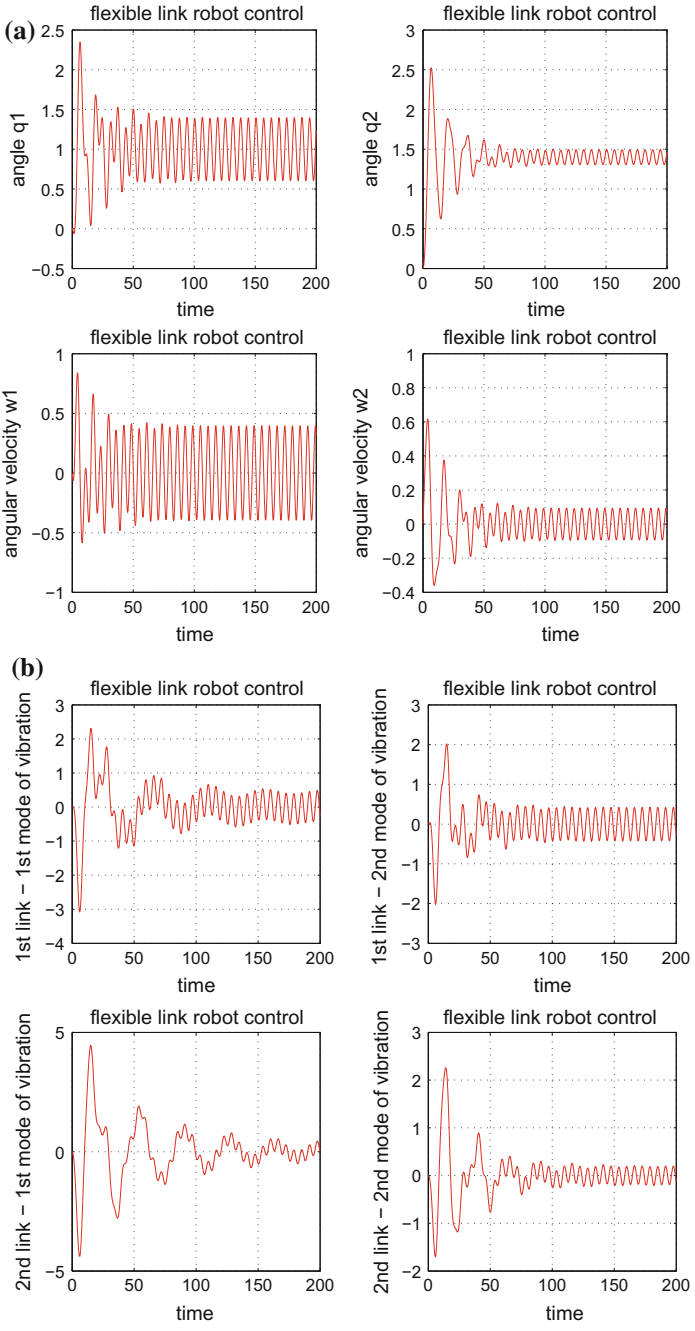

Fig. 5.4 Model-based control of a 2-link flexible robot in the presence of additive motor-torques disturbances **a** joints' angles and joints' angular velocity, **b** the first two vibration modes for each link

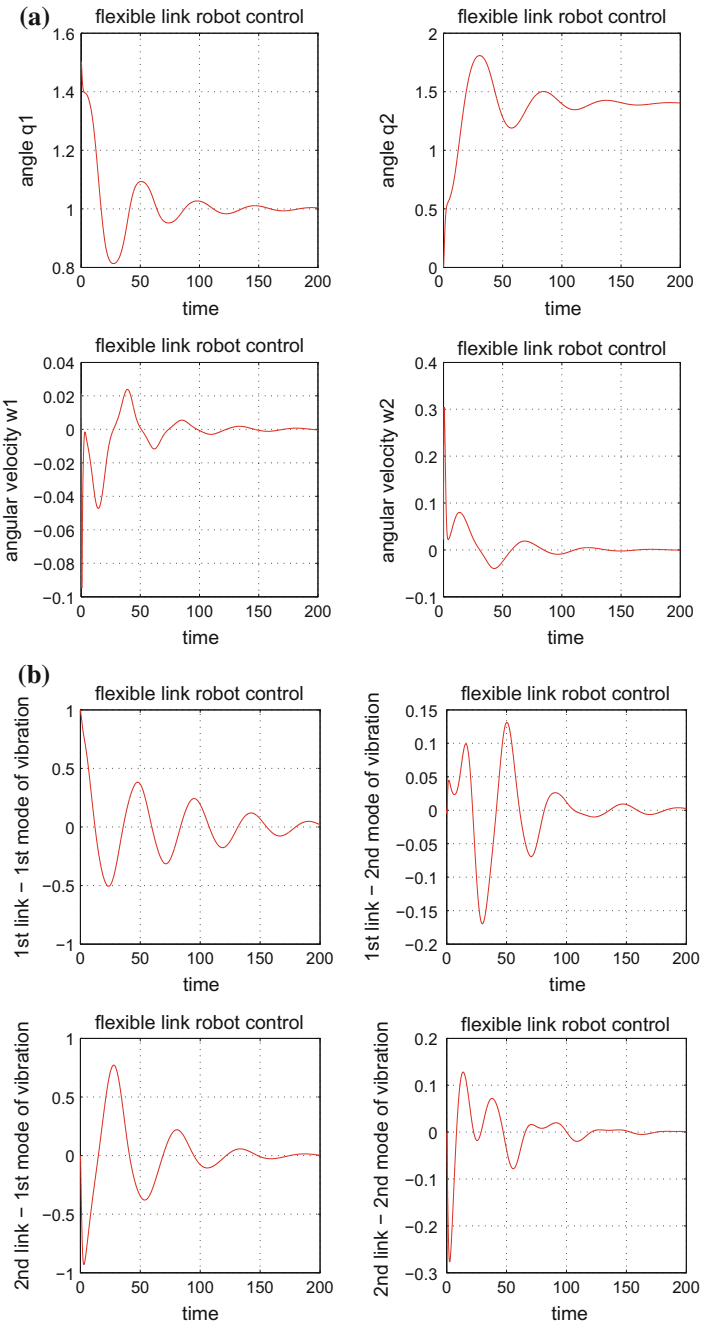

Fig. 5.5 Energy-based control of a 2-link flexible robot **a** joints' angles and joints' angular velocity, **b** the first two vibration modes for each link

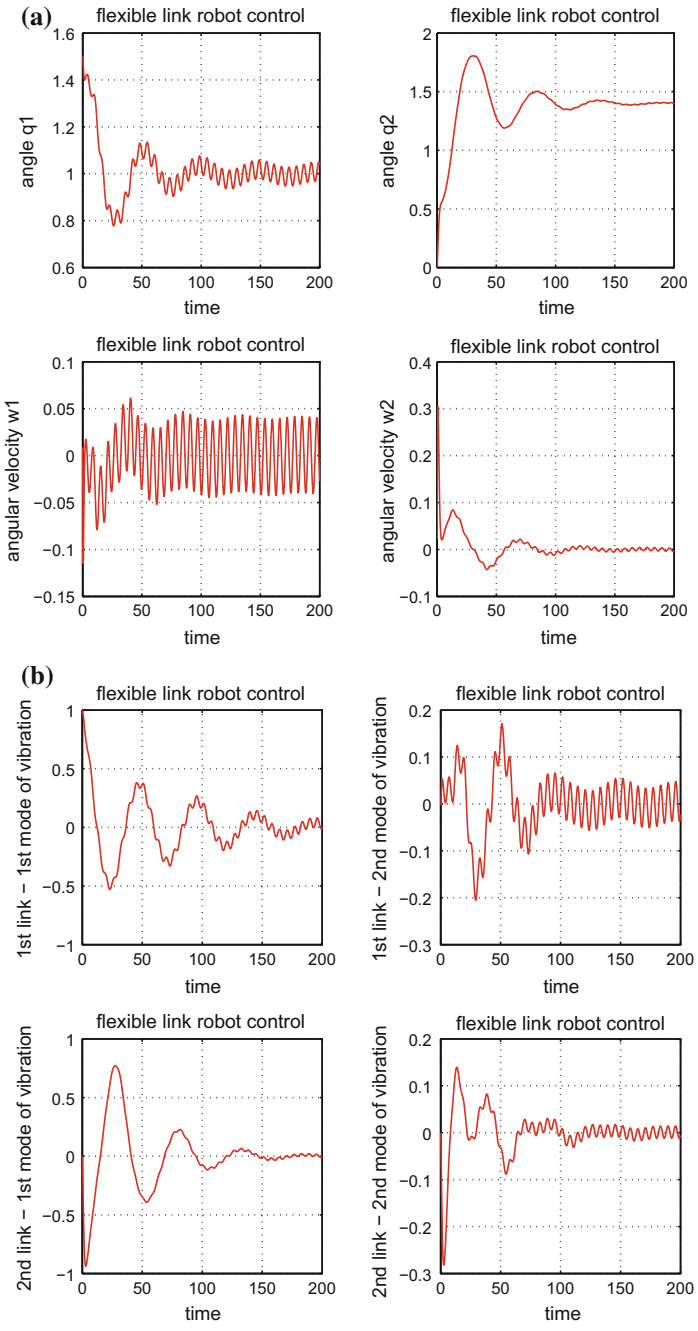

Fig. 5.6 Energy-based control of a 2-link flexible robot in the presence of additive motor-torques disturbances **a** joints' angles and joints' angular velocity, **b** the first two vibration modes for each link

to the dynamic model of rigid-link robots the dynamic model of flexible-link robots is an infinite dimensional one. As in the case of the rigid-link robot there is a certain number of mechanical degrees of freedom associated to the rotational motion of the robot's joints and there is also an infinite number of degrees of freedom associated to the vibration modes in which the deformation of the flexible link is decomposed [441]. The controller of a flexible manipulator must achieve the same motion objectives as in the case of a rigid manipulator, i.e. tracking of specific joints position and velocity setpoints. Additionally, it must also stabilize and asymptotically eliminate the vibrations of the flexible-links that are naturally excited by the joints rotational motion.

It has already been shown that the inverse dynamics model-based control for flexible-link robots relies on modal analysis, i.e. on the assumption that the deformation of the flexible link can be written as a finite series expansion containing the elementary vibration modes. However, this inverse-dynamics model-based control may result into unsatisfactory performance when an accurate model is unavailable, due to parameters uncertainty or truncation of high order vibration modes in the model [441]. Moreover, based on the state space formulation, the sliding mode control, which belongs to the wider class of the variable structure control schemes, is a nonlinear robust controller suitable for flexible-link manipulators. Sliding-mode control (SMC) can achieve simultaneous convergence of the flexible robot's joints angles and angular velocities to the desirable setpoints and efficient suppression of the flexible links vibrations. The inclusion of a switching control term in a sliding mode controller can provide robustness against parametric uncertainties and input disturbances [136, 229, 330].

As mentioned, sliding-mode control is a state-feedback based controller and its implementation requires knowledge of the complete state vector of the controlled system [204, 490]. However, there are certain elements in the state vector of the flexible-link robot which are difficult to measure, e.g. the vibration modes. Therefore, to apply sliding-mode control to the flexible manipulator it is necessary to use some kind of state estimator which can reconstruct the robot's state vector through the processing of measurements from a limited number of sensors, e.g. angles of the joints and the associated angular velocities [31, 361]. The Kalman Filter can provide real-time estimates of the state vector of the flexible link robot while assuring the optimality of estimation in the presence of measurement noises [222, 431].

Indicative results about filtering-based control for flexible-link robots can be noted. In [174] state feedback control for a flexible-link robot is implemented with the use of a state vector that is estimated through Kalman Filtering. Using fuzzy rules, an online adaptation of the covariance matrix of the Kalman Filter is performed which aims at improving the vibration suppression capabilities of the filtering-based control. In [290] a controller that follows the principles of singular perturbations theory is developed and the flexible-link robot model is decomposed into a fast and a slow dynamics subsystem. Then a two-time scale Kalman filter is designed for estimating the components of the robot's state vector associated both with the rigid (slow) and the flexible (fast) dynamics of the robot. The estimated state vector is used in the control loop. In [353] an observer-based control scheme for flexible-link

robots is developed where a fixed-gain state estimator processes measurements of the flexible-links' deformation. Lyapunov-like stability analysis is used to demonstrate the efficiency of the feedback control scheme. In [391] a method is proposed for improving the performance of flexible manipulators through the employment of robust state estimation techniques. The method is based on discrete-time Kalman filtering and sliding mode principles and is applied to the model of a 1-DOF flexible-link manipulator. Finally, in [25] the Extended Kalman Filter is redesigned in the form of a disturbance observer to estimate the disturbance forces that are exerted on the end-effector of a single-link flexible robotic manipulator. The forces' estimates provided by the filter are used in the robot's feedback control loop.

In this section it will be shown how a suitable formulation of the dynamic model of the flexible manipulator enables the application of the Kalman Filter recursion and provides accurate estimates of the robot's state vector which in turn can be used by a sliding-mode control loop. The present section extends and elaborates on the results of [437]. The performance of the proposed Kalman Filter-based sliding mode controller is also compared against the previously analyzed inverse dynamics control for flexible-link robots. As already discussed, in the latter method, by assuming a finite number of vibration modes, acontrol input is developed which inverts the dynamics of robotic system and eliminates the tracking error of its state variables [450, 583]. The evaluation of Kalman filter-based sliding-mode control against inverse dynamics control derives useful results on the efficiency of this control approach.

5.3.2 *Design of a Sliding-Mode Controller*

Sliding-mode control for flexible-link robots has been studied in several papers [136, 490]. In the sequel and for simplifying the presentation of the control scheme a 2-link flexible manipulator will be assumed, i.e. $n = 2$. The flexible-link robot model of Eq. (5.4) can be written as

$$\begin{pmatrix} \ddot{\theta} \\ \ddot{v} \end{pmatrix} = -\begin{pmatrix} M_{11} & M_{12} \\ M_{21} & M_{22} \end{pmatrix}^{-1} \{ \begin{pmatrix} 0 & 0 \\ 0 & D \end{pmatrix} \begin{pmatrix} \dot{\theta} \\ \dot{v} \end{pmatrix} + \begin{pmatrix} 0 & 0 \\ 0 & K \end{pmatrix} \begin{pmatrix} \theta \\ v \end{pmatrix} + + \begin{pmatrix} F_1 \\ F_2 \end{pmatrix} + \begin{pmatrix} G_1 \\ G_2 \end{pmatrix} - \begin{pmatrix} T \\ 0 \end{pmatrix} \} \tag{5.60}$$

The model of the flexible-link robot dynamics is written in state-space form after defining the following state vector:

$$x = [\theta_1, \theta_2, v_{11}, v_{12}, v_{21}, v_{22}, \dot{\theta}_1, \dot{\theta}_2, \dot{v}_{11}, \dot{v}_{12}, \dot{v}_{21}, \dot{v}_{22}]^T \tag{5.61}$$

The following notation is used for the inverse of the inertia matrix of the flexible-link robot

$$\begin{pmatrix} M_{11} & M_{12} \\ M_{21} & M_{22} \end{pmatrix}^{-1} = \begin{pmatrix} N_{11} & N_{12} \\ N_{21} & N_{22} \end{pmatrix} \tag{5.62}$$

where $N_{11} \in R^{2\times 2}$, $N_{12} \in R^{2\times 4}$, $N_{21} \in R^{4\times 2}$ and $N_{22} \in R^{4\times 4}$. It holds that

$$\ddot{\theta} = -N_{12}Kv - N_{12}D\dot{v} - N_{11}F_1 - N_{11}G_1 + N_{11}T \tag{5.63}$$

The elements of the damping matrix $D \in R^{4\times 4}$ are denoted as $D(i, j)$, where $D(i, j) \neq 0$ for $i = j$, while the elements of the stiffness matrix $K \in R^{4\times 4}$ are denoted as $K(i, j)$, where $K(i, j) \neq 0$ for $i = j$. Additionally the terms of the Coriolis and the gravitational vectors are $F = \left(F_1 \in R^{2\times 1},\ F_2 \in R^{4\times 1}\right)^T$ and $G = \left(G_1 \in R^{2\times 1},\ G_2 \in R^{4\times 1}\right)^T$. To obtain a more compact mathematical description in the design of the controller, and without loss of generality, in the rest of this section it will be considered that $F_2 = 0_{4\times 1}$ and $G_2 = 0_{4\times 1}$.

Therefore, one can write the dynamics of the joints of the flexible-link robot in a matrix form:

$$\begin{aligned} \ddot{x}_1 &= f_1(x) + g_1(x)u \\ \ddot{x}_2 &= f_2(x) + g_2(x)u \end{aligned} \tag{5.64}$$

where $u = \left(T_1\ T_2\right)^T$, $g_1(x) = \left(N_{11}(1, 1)\ N_{11}(1, 2)\right)$, $g_2(x) = \left(N_{11}(2, 1)\ N_{11}(2, 2)\right)$, while functions $f_1(x)$ and $f_2(x)$ are defined as

$$\begin{aligned} f_1(x) = \ & -N_{12}(1, 1)K(1, 1)x_3 - N_{12}(1, 2)K(2, 2)x_4 \\ & -N_{12}(1, 3)K(3, 3)x_5 - N_{12}(1, 4)K(4, 4)x_6 \\ & -N_{12}(1, 1)D(1, 1)x_9 - N_{12}(1, 2)D(2, 2)x_{10} \\ & -N_{12}(1, 3)D(3, 3)x_{11} - N_{12}(1, 4)D(4, 4)x_{12} \\ & -N_{11}(1, 1)F_1(1, 1) - N_{11}(1, 2)F_1(2, 1) \\ & -N_{11}(1, 1)G_1(1, 1) - N_{11}(1, 2)G_1(2, 1) \end{aligned} \tag{5.65}$$

$$\begin{aligned} f_2(x) = \ & -N_{12}(2, 1)K(1, 1)x_3 - N_{12}(2, 2)K(2, 2)x_4 \\ & -N_{12}(2, 3)K(3, 3)x_5 - N_{12}(2, 4)K(4, 4)x_6 \\ & -N_{12}(2, 1)D(1, 1)x_9 - N_{12}(2, 2)D(2, 2)x_{10} \\ & -N_{12}(2, 3)D(3, 3)x_{11} - N_{12}(2, 4)D(4, 4)x_{12} \\ & -N_{11}(2, 1)F_1(1, 1) - N_{11}(2, 2)F_1(2, 1) \\ & -N_{11}(2, 1)G_1(1, 1) - N_{11}(2, 2)G_1(2, 1) \end{aligned} \tag{5.66}$$

In the equations describing the joint dynamics the terms $g_1(x)$ and $g_2(x)$ depend on the elements of the inertia matrix of the flexible-link robot and are considered to be known. On the other hand, the terms $f_1(x)$ and $f_2(x)$ are considered to vary in uncertainty ranges, given by

$$|f_1 - \hat{f}_1| \leq \Delta F_1,\ |f_2 - \hat{f}_2| \leq \Delta F_2 \tag{5.67}$$

The following tracking error for the joints angles is defined:

$$e_1 = x_1 - x_1^d,\ e_2 = x_2 - x_2^d \tag{5.68}$$

The flexible-link robot's description given in Eq. (5.64) is in the input-output linear form and signifies also that the robotic system can be written in a canonical state-space form. Moreover, the sliding surface vector $s = [s_1, s_2]^T$ is defined with elements

$$s_1 = \dot{e}_1 + \lambda_1 e_1,\ s_2 = \dot{e}_2 + \lambda_2 e_2 \tag{5.69}$$

To achieve convergence of the tracking error to zero for the ith element of the state vector the following conditions should hold:

$$\frac{1}{2}\frac{d}{dt}s_i^2 \leq -\eta_i |s_i|,\quad \eta_i > 0,\quad i = 1, 2 \tag{5.70}$$

The sliding-mode control law is finally given by

$$u = \begin{pmatrix} g_1(x) \\ g_2(x) \end{pmatrix}^{-1} \cdot\cdot \begin{pmatrix} \ddot{x}_1^d - \hat{f}_1(x) - \lambda_1(\dot{x}_1 - \dot{x}_1^d) - k_1 sgn(s_1) \\ \ddot{x}_2^d - \hat{f}_2(x) - \lambda_2(\dot{x}_2 - \dot{x}_2^d) - k_2 sgn(s_2) \end{pmatrix} \tag{5.71}$$

To define the permissible values for the switching gains k_i $i = 1, 2$ the following conditions are used

$$\begin{gathered} \tfrac{1}{2}\tfrac{d}{dt}s_i^2 \leq -\eta_i |s_i| \Rightarrow s_i \dot{s}_i \leq -\eta_i |s_i| \Rightarrow \\ \left[f_i(x) + g_i(x)u - \ddot{x}_i^d + \lambda_i(\dot{x}_i - \dot{x}_i^d) \right] s_i \leq -\eta_i |s_i| \end{gathered} \tag{5.72}$$

The conditions given in Eq. (5.72) can be written as follows

$$\begin{gathered} \begin{pmatrix} s_1 & 0 \\ 0 & s_2 \end{pmatrix} \{ \begin{pmatrix} f_1(x) \\ f_2(x) \end{pmatrix} + \begin{pmatrix} g_1(x) \\ g_2(x) \end{pmatrix} u - \begin{pmatrix} \ddot{x}_1^d \\ \ddot{x}_2^d \end{pmatrix} + \\ + \begin{pmatrix} \lambda_1(\dot{x}_1 - \dot{x}_1^d) \\ \lambda_2(\dot{x}_2 - \dot{x}_2^d) \end{pmatrix} \} \leq \begin{pmatrix} -\eta_1 |s_1| \\ -\eta_2 |s_2| \end{pmatrix} \end{gathered} \tag{5.73}$$

Substituting in Eq. (5.73) the control law u that was calculated in Eq. (5.71), one obtains

$$\begin{pmatrix} s_1 & 0 \\ 0 & s_2 \end{pmatrix} \begin{pmatrix} f_1(x) - \hat{f}_1(x) - k_1 sgn(s_1) \\ f_2(x) - \hat{f}_2(x) - k_2 sgn(s_2) \end{pmatrix} \leq \begin{pmatrix} -\eta_1 |s_1| \\ -\eta_2 |s_2| \end{pmatrix} \tag{5.74}$$

or equivalently

$$\begin{gathered} (f_1(x) - \hat{f}_1(x) - k_1 sgn(s_1)) s_1 \leq -\eta_1 |s_1| \\ (f_2(x) - \hat{f}_2(x) - k_2 sgn(s_2)) s_2 \leq -\eta_2 |s_2| \end{gathered} \tag{5.75}$$

and using Eq. (5.67) one has

$$\begin{gathered} \Delta F_1 s_1 - k_1 sgn(s_1) s_1 \leq -\eta_1 |s_1| \\ \Delta F_2 s_2 - k_2 sgn(s_2) s_2 \leq -\eta_2 |s_2| \end{gathered} \tag{5.76}$$

or equivalently

$$\begin{array}{l} \Delta F_1 s_1 - k_1 |s_1| \leq -\eta_1 |s_1| \\ \Delta F_2 s_2 - k_2 |s_2| \leq -\eta_2 |s_2| \end{array} \tag{5.77}$$

The switching control gains are chosen to satisfy

$$k_1 = \Delta F_1 + \eta_1,\ k_2 = \Delta F_2 + \eta_2 \tag{5.78}$$

Substituting Eqs. (5.78) into (5.77) gives

$$\begin{array}{l} \Delta F_1 s_1 - \Delta F_1 |s_1| - \eta_1 |s_1| \leq -\eta_1 |s_1| \\ \Delta F_2 s_2 - \Delta F_2 |s_2| - \eta_2 |s_2| \leq -\eta_2 |s_2| \end{array} \tag{5.79}$$

or equivalently

$$\begin{array}{l} \Delta F_1 s_1 \leq \Delta F_1 |s_1| \\ \Delta F_2 s_2 \leq \Delta F_2 |s_2| \end{array} \tag{5.80}$$

This assures that $lim_{t \to \infty} s_i = 0,\ i = 1, 2$ and consequently the asymptotic elimination of the tracking error for the joints' angle and rotation speed.

5.3.3 *Estimation of the Non-measurable State Variables*

Knowing that certain elements of the state vector of the flexible-link robot are not directly measurable, e.g. vibration modes, it becomes necessary to estimate these variables with the use of a state observer or filter. Indicative research results on state estimation-based control for flexible-link robots have been given in [31, 204, 361]. To obtain a state estimation-based control scheme for the flexible manipulator, in this section the state-space description of the flexible-link robot dynamics in the form of Eq. (5.81) is used:

$$\begin{array}{c} \dot{x} = Ax + Bu_a \\ y = Cx \end{array} \tag{5.81}$$

where $x \in R^{12 \times 1}$ is the previously defined state vector, $u_a = [T_1 - F_1 - G_1, T_2 - F_1 - G_1]^T$, while matrices A and B are defined as

$$A = \begin{pmatrix} 0_{6\times 6} & I_{6\times 6} \\ [0_{2\times 2}, -N_{12}K] & [0_{2\times 2}, -N_{12}D] \\ [0_{4\times 2}, -N_{22}K] & [0_{4\times 2}, -N_{22}D] \end{pmatrix} \quad B = \begin{pmatrix} 0_{6\times 2} \\ N_{12} \\ N_{22} \end{pmatrix} \tag{5.82}$$

$$C = \begin{pmatrix} 1 & 0 & 0_{1\times 10} \\ 0 & 1 & 0_{1\times 10} \\ 0_{1\times 6} & 1 & 0_{1\times 5} \\ 0_{1\times 7} & 1 & 0_{1\times 4} \end{pmatrix} \tag{5.83}$$

Thus, it is considered that the measurable elements of the robot's state vector are the joints' angles and the joints' angular velocities. After applying common discretization methods the linear continuous-time model of the flexible-link robot of Eq. (5.81) is turned into a discrete-time linear model, which makes use of the discrete-time equivalents of matrices A, B and C defined in Eqs. (5.82) and (5.83).

For the latter discrete-time model the application of the recursion of the discrete-time Kalman Filter is possible. The discrete-time Kalman filter can be decomposed into two parts: (i) time update (prediction stage), and (ii) measurement update (correction stage) [222, 450, 457]. The first part employs an estimate of the state vector $x(k)$ made before the output measurement $y(k)$ is available (a priori estimate). The second part estimates $x(k)$ after $y(k)$ has become available (a posteriori estimate). The covariance matrices associated with $\hat{x}^-(k)$ and $\hat{x}(k)$ are defined as: $P^-(k) = Cov[e^-(k)] = E[e^-(k)e^-(k)^T]$ and $P(k) = Cov[e(k)] = E[e(k)e^T(k)]$.

Matrices A, B and C of the linear state-space model are defined in Eq. (5.82) and Eq. (5.83). Next, by applying common discretization methods (e.g. Tustin transform) the continuous-time linear model of the robot's dynamics is transformed into a linear discrete-time model where matrices A, B, and C are substituted by their discrete-time equivalents A_d, B_d and C_d. For this latter model, the application of the standard discrete-time Kalman Filter recursion is possible.

The recursion of the discrete-time Kalman Filter is formulated as:

measurement update:

$$\begin{aligned} K(k) &= P^-(k)C_d(k)^T[C_d(k)\cdot P^-(k)C_d(k)^T + R]^{-1} \\ \hat{x}(k) &= \hat{x}^-(k) + K(k)[y(k) - C_d(k)\hat{x}^-(k)] \\ P(k) &= P^-(k) - K(k)C_d(k)P^-(k) \end{aligned} \tag{5.84}$$

time update:

$$\begin{aligned} P^-(k+1) &= A_d(k)P(k)A_d^T(k) + Q(k) \\ \hat{x}^-(k+1) &= A_d(k)\hat{x}(k) + B(_dk)u(k) \end{aligned} \tag{5.85}$$

5.3.4 Simulation Tests

5.3.4.1 Inverse Dynamics Control for a 2-Link FLR

The 2-link flexible robot of Fig. 5.1 is considered. The robot consists of two flexible links of length $L_1 = 0.45\,\text{m}$ and $L_2 = 0.45\,\text{m}$, respectively. The dynamic model of the robot is given by Eq. (5.4). The elements of the inertia matrix M are:

$$\begin{aligned} M_{11} &= \begin{pmatrix} 1 & 2 \\ 2 & 1 \end{pmatrix}, \quad M_{22} = \begin{pmatrix} 1 & 0 \\ 0 & 1 \end{pmatrix} \\ M_{12} &= M_{21}^T = \begin{pmatrix} 1 & 1 & 0.2 & 0.3 \\ 0.5 & 0.1 & 2 & 0.7 \end{pmatrix} \end{aligned} \tag{5.86}$$

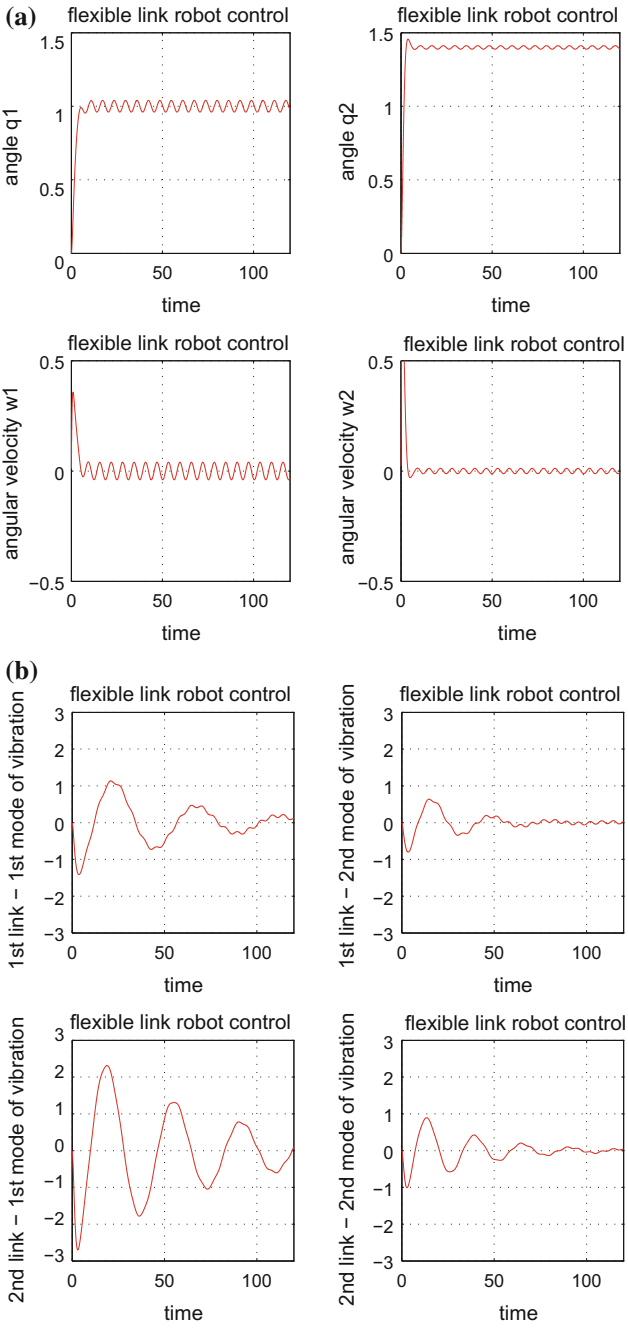

Fig. 5.7 **a** Inverse dynamics control of a 2-link flexible robot under additive motor-torques disturbances: joints' angles (rad) and joints' angular velocity (rad/sec) **b** Inverse dynamics control of a 2-link flexible robot under additive motor-torques disturbances: the first two vibration modes for each link

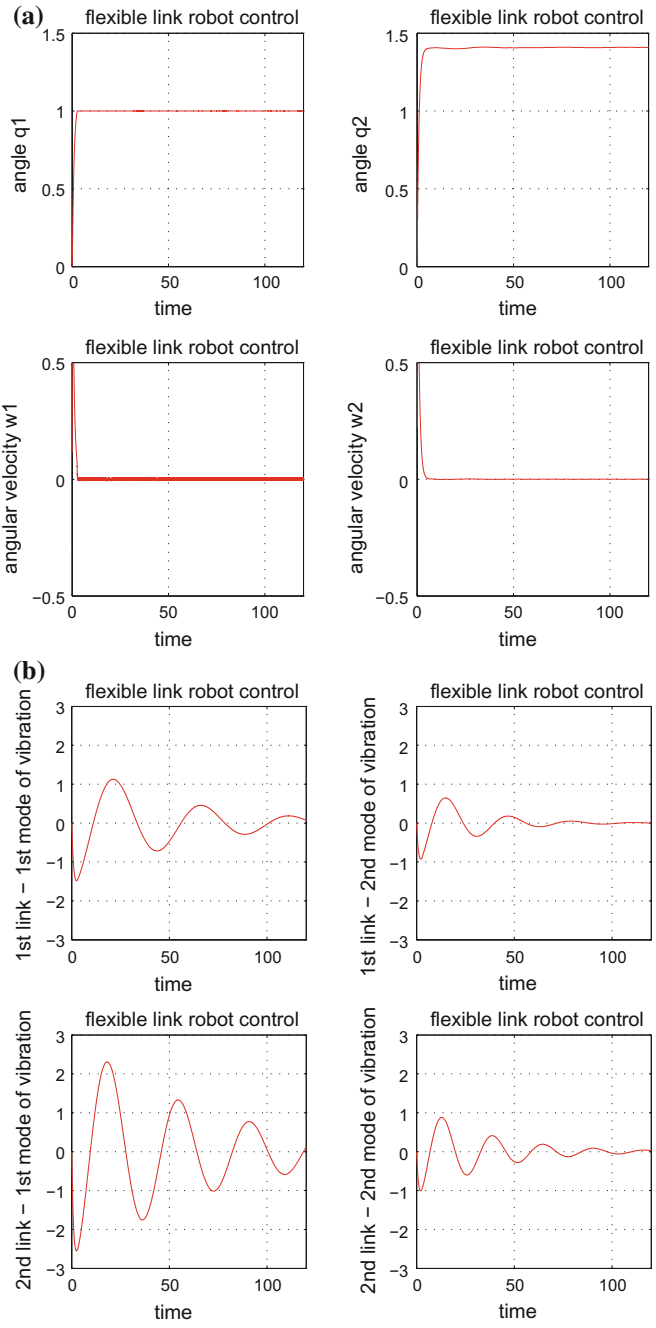

Fig. 5.8 **a** Sliding-mode control of a 2-link flexible robot under additive motor-torques disturbances: joints' angles (rad) and joints' angular velocity (rad/sec) for each link, **b** Sliding-mode control of a 2-link flexible robot under additive motor-torques disturbances: the first two vibration modes for each link

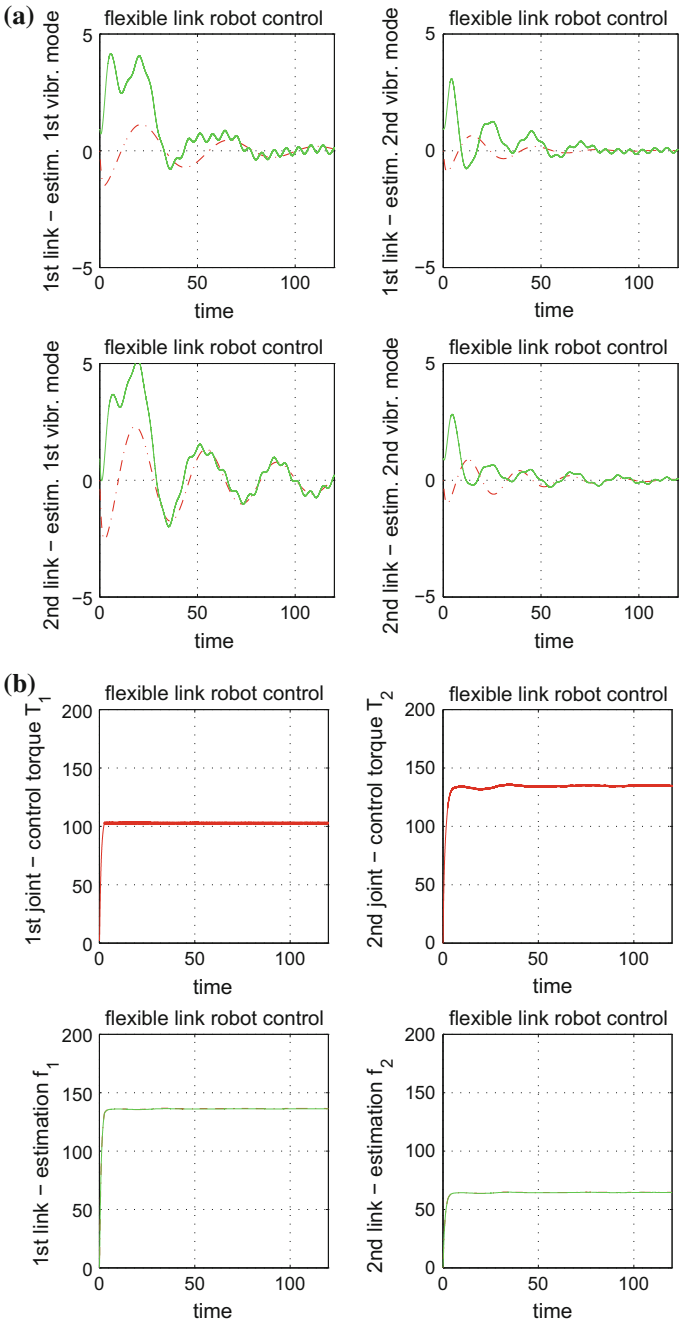

Fig. 5.9 **a** Estimates (continuous lines) of the non-measurable state vector elements of the flexible-link robot (vibration modes), provided by the Kalman Filter. **b** Top row: Control inputs (torques) $T_i,\ i = 1, 2$ applied to the joints of the flexible-link robot, Bottom row: estimation of function $f_i,\ i = 1, 2$ of the flexible-link dynamics

The damping matrix is $D = diag\{0.04, 0.08, 0.03, 0.06\}$ while the stiffness matrix is $K = diag\{0.02, 0.04, 0.03, 0.06\}$. The inverse dynamics control law given in Sect. 5.2.2 was employed. The selection of the gain matrices K_p and K_d determines the transient response of the closed loop system. The following controller gains have been considered: $K_p = diag\{10.5, 15.5\}$ and $K_d = diag\{10.9, 15.0\}$. The desirable joints' positions were $\theta_{d_1} = 1$ rad and $\theta_{d_2} = 1.4$ rad. It was considered that an additive disturbance torque $d_i(t) = 0.3cos(t)$ affected each joint.

In the simulation diagrams about angular position and velocity setpoint tracking, the horizontal axis represents time in sec, and since the robot's control takes place in the configuration space the vertical axis represents angle in rad and angular velocity in rad/sec. Moreover, as shown in Eq. (5.3), the vibration modes variables $v_i(t)$ are functions of time and are associated with the deformation of the flexible links $w(x, t)$. The performance of the model-based controller of the flexible-link robot in the presence of disturbance is depicted in Fig. 5.7. It can be seen that vibrations around the desirable joint positions cannot be eliminated.

5.3.4.2 Sliding-Mode Control for a 2-Link Flexible-Link Robot

The sliding-mode control scheme proposed in Sect. 5.3.2 was tested on the 2-link flexible robotic manipulator model. It was assumed that the complete state vector of the robot was not directly measurable. Thus, it was considered that only the joints' angles $\theta_i,\ i = 1, 2$ and the associated angular velocities $\dot{\theta}_i,\ i = 1, 2$ could be obtained through sensor measurements, whereas the vibration modes of the links $v_{11}, v_{12}, v_{21}, v_{22}$ were not measurable and had to be reconstructed with the use of the Kalman Filter.

The obtained results are depicted in Fig. 5.8a where convergence of the joints' angles and velocities to the desirable setpoints is shown. In Fig. 5.8b the evolution in time of the vibration modes of the flexible links is presented. Figure 5.9a presents the estimation of the flexible-links' vibration modes, provided by the Kalman Filter. It can be noticed that the Kalman Filter state estimates track with satisfactory accuracy the real values of the non-measurable state vector elements. Finally, Fig. 5.9b depicts the control inputs (torques) applied to the joints of the flexible-link robot.

From the simulation experiments it can be noticed that as the Kalman Filter-based sliding-mode controller, the energy-based controller is also efficient in controlling the position and in suppressing vibrations of the flexible links. However, an advantage of the Kalman Filter-based sliding mode control is that it achieves accurate tracking for any type of joint angle and velocity set-point whereas the convergence of the energy-based control is assured only in the case of constant set-points.